

Measurements of the branching fractions of $\Lambda_c^+ \rightarrow p\eta$ and $\Lambda_c^+ \rightarrow p\pi^0$ decays at Belle

S. X. Li,¹² C. P. Shen,¹² I. Adachi,^{19,15} J. K. Ahn,⁴⁰ H. Aihara,⁸⁷ D. M. Asner,³ T. Aushev,²¹ R. Ayad,⁸² V. Babu,⁸ S. Bahinipati,²⁵ P. Behera,²⁸ J. Bennett,⁵³ F. Bernlochner,² M. Bessner,¹⁸ V. Bhardwaj,²⁴ B. Bhuyan,²⁶ T. Bilka,⁵ J. Biswal,³⁵ A. Bobrov,^{4,67} A. Bozek,⁶³ T. E. Browder,¹⁸ M. Campajola,^{33,58} L. Cao,² D. Červenkov,⁵ M.-C. Chang,¹¹ A. Chen,⁶⁰ B. G. Cheon,¹⁷ K. Chilikin,⁴⁴ H. E. Cho,¹⁷ K. Cho,³⁹ Y. Choi,⁸⁰ S. Choudhury,²⁷ D. Cinabro,⁹² S. Cunliffe,⁸ S. Das,⁴⁹ N. Dash,²⁸ G. De Nardo,^{33,58} R. Dhamija,²⁷ F. Di Capua,^{33,58} Z. Doležal,⁵ T. V. Dong,¹² S. Eidelman,^{4,67,44} D. Epifanov,^{4,67} T. Ferber,⁸ D. Ferlewicz,⁵² B. G. Fulsom,⁶⁹ R. Garg,⁷⁰ V. Gaur,⁹¹ A. Garmash,^{4,67} A. Giri,²⁷ P. Goldenzweig,³⁶ B. Golob,^{46,35} O. Grzymkowska,⁶³ K. Gudkova,^{4,67} C. Hadjivasiliou,⁶⁹ O. Hartbrich,¹⁸ K. Hayasaka,⁶⁵ H. Hayashii,⁵⁹ M. T. Hedges,¹⁸ W.-S. Hou,⁶² C.-L. Hsu,⁸¹ T. Iijima,^{57,56} K. Inami,⁵⁶ G. Inguglia,³¹ A. Ishikawa,^{19,15} R. Itoh,^{19,15} M. Iwasaki,⁶⁸ Y. Iwasaki,¹⁹ W. W. Jacobs,²⁹ E.-J. Jang,¹⁶ S. Jia,¹² Y. Jin,⁸⁷ C. W. Joo,³⁷ K. K. Joo,⁶ A. B. Kaliyar,⁸³ K. H. Kang,⁴² G. Karyan,⁸ Y. Kato,⁵⁶ T. Kawasaki,³⁸ H. Kichimi,¹⁹ B. H. Kim,⁷⁶ C. H. Kim,¹⁷ D. Y. Kim,⁷⁹ K.-H. Kim,⁹⁴ S. H. Kim,⁷⁶ Y.-K. Kim,⁹⁴ K. Kinoshita,⁷ P. Kodyš,⁵ T. Konno,³⁸ A. Korobov,^{4,67} S. Korpar,^{50,35} E. Kovalenko,^{4,67} P. Križan,^{46,35} R. Kroeger,⁵³ P. Krokovny,^{4,67} T. Kuhr,⁴⁷ M. Kumar,⁴⁹ K. Kumara,⁹² A. Kuzmin,^{4,67} Y.-J. Kwon,⁹⁴ K. Lalwani,⁴⁹ J. S. Lange,¹³ I. S. Lee,¹⁷ S. C. Lee,⁴² C. H. Li,⁴⁵ L. K. Li,⁷ Y. B. Li,⁷¹ L. Li Gioi,⁵¹ J. Libby,²⁸ K. Lieret,⁴⁷ D. Liventsev,^{92,19} M. Masuda,^{86,73} T. Matsuda,⁵⁴ D. Matvienko,^{4,67,44} M. Merola,^{33,58} F. Metzner,³⁶ R. Mizuk,^{44,21} S. Mohanty,^{83,90} T. Mori,⁵⁶ M. Nakao,^{19,15} Z. Natkaniec,⁶³ A. Natochii,¹⁸ L. Nayak,²⁷ M. Niiyama,⁴¹ N. K. Nisar,³ S. Nishida,^{19,15} H. Ono,^{64,65} Y. Onuki,⁸⁷ P. Pakhlov,^{44,55} G. Pakhlova,^{21,44} T. Pang,⁷² S. Pardi,³³ H. Park,⁴² S.-H. Park,¹⁹ S. Patra,²⁴ S. Paul,^{84,51} T. K. Pedlar,⁴⁸ R. Pestotnik,³⁵ L. E. Piilonen,⁹¹ T. Podobnik,^{46,35} V. Popov,²¹ E. Prencipe,²² M. T. Prim,² M. Röhrken,⁸ A. Rostomyan,⁸ N. Rout,²⁸ G. Russo,⁵⁸ D. Sahoo,⁸³ Y. Sakai,^{19,15} S. Sandilya,²⁷ A. Sangal,⁷ L. Santelj,^{46,35} T. Sanuki,⁸⁵ V. Savinov,⁷² G. Schnell,^{1,23} J. Schueler,¹⁸ C. Schwanda,³¹ Y. Seino,⁶⁵ K. Senyo,⁹³ M. E. Sevier,⁵² M. Shapkin,³² C. Sharma,⁴⁹ V. Shebalin,¹⁸ J.-G. Shiu,⁶² B. Shwartz,^{4,67} E. Solovieva,⁴⁴ S. Stanič,⁶⁶ M. Starič,³⁵ Z. S. Stottler,⁹¹ M. Sumihama,¹⁴ T. Sumiyoshi,⁸⁹ W. Sutcliffe,² M. Takizawa,^{77,20,74} K. Tanida,³⁴ Y. Tao,¹⁰ F. Tenchini,⁸ K. Trabelsi,⁴³ M. Uchida,⁸⁸ S. Uehara,^{19,15} T. Uglov,^{44,21} K. Uno,⁶⁵ S. Uno,^{19,15} P. Urquijo,⁵² R. Van Tonder,² G. Varner,¹⁸ A. Vossen,⁹ C. H. Wang,⁶¹ E. Wang,⁷² M.-Z. Wang,⁶² P. Wang,³⁰ S. Watanuki,⁴³ E. Won,⁴⁰ X. Xu,⁷⁸ B. D. Yabsley,⁸¹ W. Yan,⁷⁵ S. B. Yang,⁴⁰ H. Ye,⁸ J. Yelton,¹⁰ J. H. Yin,⁴⁰ C. Z. Yuan,³⁰ Y. Yusa,⁶⁵ Z. P. Zhang,⁷⁵ V. Zhilich,^{4,67} V. Zhukova,⁴⁴ and V. Zhulanov,^{4,67}

(The Belle Collaboration)

¹Department of Physics, University of the Basque Country UPV/EHU, 48080 Bilbao

²University of Bonn, 53115 Bonn

³Brookhaven National Laboratory, Upton, New York 11973

⁴Budker Institute of Nuclear Physics SB RAS, Novosibirsk 630090

⁵Faculty of Mathematics and Physics, Charles University, 121 16 Prague

⁶Chonnam National University, Gwangju 61186

⁷University of Cincinnati, Cincinnati, Ohio 45221

⁸Deutsches Elektronen-Synchrotron, 22607 Hamburg

⁹Duke University, Durham, North Carolina 27708

¹⁰University of Florida, Gainesville, Florida 32611

¹¹Department of Physics, Fu Jen Catholic University, Taipei 24205

¹²Key Laboratory of Nuclear Physics and Ion-beam Application (MOE) and Institute of Modern Physics, Fudan University, Shanghai 200443

¹³Justus-Liebig-Universität Gießen, 35392 Gießen

¹⁴Gifu University, Gifu 501-1193

¹⁵SOKENDAI (The Graduate University for Advanced Studies), Hayama 240-0193

¹⁶Gyeongsang National University, Jinju 52828

¹⁷Department of Physics and Institute of Natural Sciences, Hanyang University, Seoul 04763

¹⁸University of Hawaii, Honolulu, Hawaii 96822

¹⁹High Energy Accelerator Research Organization (KEK), Tsukuba 305-0801

²⁰J-PARC Branch, KEK Theory Center, High Energy Accelerator Research Organization (KEK), Tsukuba 305-0801

²¹Higher School of Economics (HSE), Moscow 101000

²²Forschungszentrum Jülich, 52425 Jülich

²³IKERBASQUE, Basque Foundation for Science, 48013 Bilbao

- ²⁴Indian Institute of Science Education and Research Mohali, SAS Nagar, 140306
- ²⁵Indian Institute of Technology Bhubaneswar, Satya Nagar 751007
- ²⁶Indian Institute of Technology Guwahati, Assam 781039
- ²⁷Indian Institute of Technology Hyderabad, Telangana 502285
- ²⁸Indian Institute of Technology Madras, Chennai 600036
- ²⁹Indiana University, Bloomington, Indiana 47408
- ³⁰Institute of High Energy Physics, Chinese Academy of Sciences, Beijing 100049
- ³¹Institute of High Energy Physics, Vienna 1050
- ³²Institute for High Energy Physics, Protvino 142281
- ³³INFN—Sezione di Napoli, 80126 Napoli
- ³⁴Advanced Science Research Center, Japan Atomic Energy Agency, Naka 319-1195
- ³⁵J. Stefan Institute, 1000 Ljubljana
- ³⁶Institut für Experimentelle Teilchenphysik, Karlsruher Institut für Technologie, 76131 Karlsruhe
- ³⁷Kavli Institute for the Physics and Mathematics of the Universe (WPI), University of Tokyo, Kashiwa 277-8583
- ³⁸Kitasato University, Sagami-hara 252-0373
- ³⁹Korea Institute of Science and Technology Information, Daejeon 34141
- ⁴⁰Korea University, Seoul 02841
- ⁴¹Kyoto Sangyo University, Kyoto 603-8555
- ⁴²Kyungpook National University, Daegu 41566, South
- ⁴³Université Paris-Saclay, CNRS/IN2P3, IJCLab, 91405 Orsay
- ⁴⁴P. N. Lebedev Physical Institute of the Russian Academy of Sciences, Moscow 119991
- ⁴⁵Liaoning Normal University, Dalian 116029
- ⁴⁶Faculty of Mathematics and Physics, University of Ljubljana, 1000 Ljubljana
- ⁴⁷Ludwig Maximilians University, 80539 München
- ⁴⁸Luther College, Decorah, Iowa 52101
- ⁴⁹Malaviya National Institute of Technology Jaipur, Jaipur 302017
- ⁵⁰University of Maribor, 2000 Maribor
- ⁵¹Max-Planck-Institut für Physik, 80805 München
- ⁵²School of Physics, University of Melbourne, Victoria 3010
- ⁵³University of Mississippi, University, Mississippi 38677
- ⁵⁴University of Miyazaki, Miyazaki 889-2192
- ⁵⁵Moscow Physical Engineering Institute, Moscow 115409
- ⁵⁶Graduate School of Science, Nagoya University, Nagoya 464-8602
- ⁵⁷Kobayashi-Maskawa Institute, Nagoya University, Nagoya 464-8602
- ⁵⁸Università di Napoli Federico II, 80126 Napoli
- ⁵⁹Nara Women's University, Nara 630-8506
- ⁶⁰National Central University, Chung-li 32054
- ⁶¹National United University, Miao Li 36003
- ⁶²Department of Physics, National Taiwan University, Taipei 10617
- ⁶³H. Niewodniczanski Institute of Nuclear Physics, Krakow 31-342
- ⁶⁴Nippon Dental University, Niigata 951-8580
- ⁶⁵Niigata University, Niigata 950-2181
- ⁶⁶University of Nova Gorica, 5000 Nova Gorica
- ⁶⁷Novosibirsk State University, Novosibirsk 630090
- ⁶⁸Osaka City University, Osaka 558-8585
- ⁶⁹Pacific Northwest National Laboratory, Richland, Washington 99352
- ⁷⁰Panjab University, Chandigarh 160014
- ⁷¹Peking University, Beijing 100871
- ⁷²University of Pittsburgh, Pittsburgh, Pennsylvania 15260
- ⁷³Research Center for Nuclear Physics, Osaka University, Osaka 567-0047
- ⁷⁴Meson Science Laboratory, Cluster for Pioneering Research, RIKEN, Saitama 351-0198
- ⁷⁵Department of Modern Physics and State Key Laboratory of Particle Detection and Electronics, University of Science and Technology of China, Hefei 230026
- ⁷⁶Seoul National University, Seoul 08826
- ⁷⁷Showa Pharmaceutical University, Tokyo 194-8543
- ⁷⁸Soochow University, Suzhou 215006
- ⁷⁹Soongsil University, Seoul 06978
- ⁸⁰Sungkyunkwan University, Suwon 16419

⁸¹*School of Physics, University of Sydney, New South Wales 2006*⁸²*Department of Physics, Faculty of Science, University of Tabuk, Tabuk 71451*⁸³*Tata Institute of Fundamental Research, Mumbai 400005*⁸⁴*Department of Physics, Technische Universität München, 85748 Garching*⁸⁵*Department of Physics, Tohoku University, Sendai 980-8578*⁸⁶*Earthquake Research Institute, University of Tokyo, Tokyo 113-0032*⁸⁷*Department of Physics, University of Tokyo, Tokyo 113-0033*⁸⁸*Tokyo Institute of Technology, Tokyo 152-8550*⁸⁹*Tokyo Metropolitan University, Tokyo 192-0397*⁹⁰*Utkal University, Bhubaneswar 751004*⁹¹*Virginia Polytechnic Institute and State University, Blacksburg, Virginia 24061*⁹²*Wayne State University, Detroit, Michigan 48202*⁹³*Yamagata University, Yamagata 990-8560*⁹⁴*Yonsei University, Seoul 03722*

(Received 24 February 2021; accepted 18 March 2021; published 14 April 2021)

We report measurements of the branching fractions of singly Cabibbo-suppressed decays $\Lambda_c^+ \rightarrow p\eta$ and $\Lambda_c^+ \rightarrow p\pi^0$ using the full Belle data sample corresponding to an integrated luminosity of 980.6 fb^{-1} . The data were collected by the Belle detector at the KEKB e^+e^- asymmetric energy collider. A clear Λ_c^+ signal is seen in the invariant mass distribution of $p\eta$. The fitted number of signal events of the $\Lambda_c^+ \rightarrow p\eta$ process is 7734 ± 263 ; from this, we measure the ratio of branching fractions $\mathcal{B}(\Lambda_c^+ \rightarrow p\eta)/\mathcal{B}(\Lambda_c^+ \rightarrow pK^-\pi^+) = [2.258 \pm 0.077(\text{stat}) \pm 0.122(\text{syst})] \times 10^{-2}$, from which we infer the branching fraction $\mathcal{B}(\Lambda_c^+ \rightarrow p\eta) = [1.42 \pm 0.05(\text{stat}) \pm 0.11(\text{syst})] \times 10^{-3}$. In addition, no significant signal for $\Lambda_c^+ \rightarrow p\pi^0$ is found, so an upper limit on the branching fraction of $\mathcal{B}(\Lambda_c^+ \rightarrow p\pi^0) < 8.0 \times 10^{-5}$ at a 90% credibility level is set, more than 3 times better than the best current upper limit.

DOI: [10.1103/PhysRevD.103.072004](https://doi.org/10.1103/PhysRevD.103.072004)

I. INTRODUCTION

Weak decays of charmed baryons are useful for testing many contradictory theoretical models and methods—e.g., the flavor symmetry approach and heavy quark effective theory [1–4]. In contrast with the decays of charmed mesons, the decays of some charmed baryons are helicity suppressed, making the W -boson exchange favored [5]. The understanding of charmed baryons has progressed relatively slowly compared to that of charmed mesons. The main reason is that the cross section for the generation of charmed baryons is smaller than that of the mesons, so that some reactions with small decay branching fractions are difficult to observe experimentally [6–8]. Although there have been many improved measurements of the properties of charmed baryons, precision measurements of the decay branching fractions still remain poor for many Cabibbo-favored (CF) decay modes and even worse for some decay modes dominated by Cabibbo suppression and W -boson exchange [9].

In theory, the singly Cabibbo-suppressed (SCS) decays $\Lambda_c^+ \rightarrow p\pi^0$ and $\Lambda_c^+ \rightarrow p\eta$ proceed predominantly through

internal W emission and W exchange. Typical decay diagrams of two SCS decays are shown in Fig. 1. The internal W emission involving an s quark in Fig. 1(f) is allowed in $\Lambda_c^+ \rightarrow p\eta$ but absent in $\Lambda_c^+ \rightarrow p\pi^0$. The theoretical calculations predict the branching fraction of $\Lambda_c^+ \rightarrow p\eta$ to be at least an order of magnitude greater than that of $\Lambda_c^+ \rightarrow p\pi^0$ and give different assumption-dependent results for the branching fractions of these SCS decays [1,3,10–12]. In contrast with the strong decays of heavy-flavor mesons, the W -boson exchange mechanism plays an important role in the decay of charmed baryons. Thus, measuring the branching fractions of these two SCS decays will help elucidate the decay mechanism of charmed baryons.

The first evidence for the decay $\Lambda_c^+ \rightarrow p\eta$ with a statistical significance of 4.2σ and a branching fraction of $\mathcal{B}(\Lambda_c^+ \rightarrow p\eta) = (1.24 \pm 0.30) \times 10^{-3}$ was reported by the BESIII Collaboration [13]. They found no significant $\Lambda_c^+ \rightarrow p\pi^0$ signal and set an upper limit on its branching fraction $\mathcal{B}(\Lambda_c^+ \rightarrow p\pi^0) < 2.7 \times 10^{-4}$ at a 90% confidence level [13].

To improve the measurement precision, we measure the ratio of the branching fractions of the two SCS processes with respect to the CF $\Lambda_c^+ \rightarrow pK^-\pi^+$ decay mode:

$$\frac{\mathcal{B}(\text{SCS})}{\mathcal{B}(\text{CF})} = \frac{N^{\text{obs}}(\text{SCS})}{\epsilon^{\text{MC}}(\text{SCS}) \times \mathcal{B}(\pi^0/\eta \rightarrow \gamma\gamma)} \times \frac{\epsilon^{\text{MC}}(\text{CF})}{N^{\text{obs}}(\text{CF})}, \quad (1)$$

Published by the American Physical Society under the terms of the [Creative Commons Attribution 4.0 International license](https://creativecommons.org/licenses/by/4.0/). Further distribution of this work must maintain attribution to the author(s) and the published article's title, journal citation, and DOI. Funded by SCOAP³.

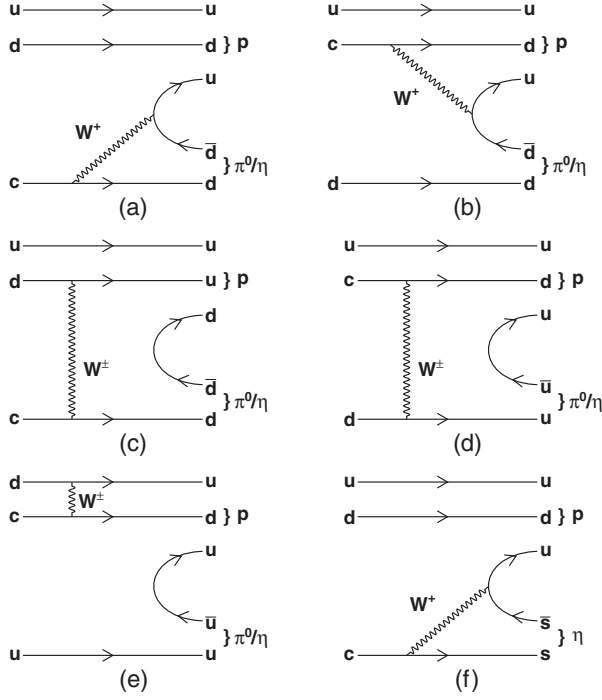


FIG. 1. Feynman diagrams for the weak Cabibbo-suppressed decays $\Lambda_c^+ \rightarrow p\pi^0$ and $\Lambda_c^+ \rightarrow p\eta$. (a),(b) internal W emission, (c), (d),(e) W exchange, and (f) internal W emission for $\Lambda_c^+ \rightarrow p\eta$.

where \mathcal{B} , ϵ^{MC} , and N^{obs} are the branching fraction, signal efficiency, and the fitted yield of signal events from data, respectively. The value of the branching fraction of the CF decay is $(6.28 \pm 0.32) \times 10^{-2}$ [9]. The values of $\mathcal{B}(\pi^0 \rightarrow \gamma\gamma)$ and $\mathcal{B}(\eta \rightarrow \gamma\gamma)$ are 0.9882 ± 0.0003 and 0.3941 ± 0.0020 , respectively [9].

II. THE DATA SAMPLE AND THE BELLE DETECTOR

The measurements of the two SCS branching fractions are based on a data sample taken at or near the $\Upsilon(1S)$, $\Upsilon(2S)$, $\Upsilon(3S)$, $\Upsilon(4S)$, and $\Upsilon(5S)$ resonances collected with the Belle detector at the KEKB asymmetric energy e^+e^- collider [14]. The integrated luminosity of the data samples is 980.6 fb^{-1} , including 711 fb^{-1} on the $\Upsilon(4S)$ resonance, 89.4 fb^{-1} off the $\Upsilon(4S)$ resonance, 121.4 fb^{-1} on the $\Upsilon(5S)$ resonance, and 58.8 fb^{-1} at the $\Upsilon(1S, 2S, 3S)$ resonances. The Belle detector is a large-solid-angle magnetic spectrometer that consists of a silicon vertex detector (SVD), a 50-layer central drift chamber (CDC), an array of aerogel threshold Cherenkov counters (ACC), a barrel-like arrangement of time-of-flight scintillation counters (TOF), and an electromagnetic calorimeter comprised of CsI(Tl) crystals (ECL) located inside a superconducting solenoid coil that provides a 1.5 T magnetic field. An iron flux return located outside of the coil is instrumented to detect K_L^0 mesons and to identify muons (KLM). The detector is described in detail elsewhere [15].

Signal MC samples of $e^+e^- \rightarrow c\bar{c}$; $c\bar{c} \rightarrow \Lambda_c^+ X$, with X denoting anything; and $\Lambda_c^+ \rightarrow pK^-\pi^+/p\pi^0/p\eta$ are used to optimize the selection criteria and estimate the reconstruction and selection efficiency, and are generated under the $\Upsilon(4S)$ resonance condition with PYTHIA [16] and EvtGen [17] and propagated with GEANT3 [18] to simulate the detector performance. The charged-conjugate modes are included unless otherwise stated.

Inclusive MC samples of $\Upsilon(4S) \rightarrow B^+B^-/B^0\bar{B}^0$, $\Upsilon(5S) \rightarrow B_s^{(*)}\bar{B}_s^{(*)}$, and $e^+e^- \rightarrow q\bar{q}$ ($q = u, d, s, c$) at $\sqrt{s} = 10.58$ and 10.867 GeV, and $\Upsilon(1S, 2S, 3S)$ decays corresponding to 2 times the integrated luminosity of each dataset are used to characterize the (potentially peaking) backgrounds [19].

III. EVENT SELECTION CRITERIA

For charged-particle tracks, the distances of closest approach with respect to the interaction point (IP) along the z axis (parallel to the positron beam) and in the transverse $r\phi$ plane are required to be less than 2.0 cm and 0.1 cm, respectively. In addition, each track is required to have at least one SVD hit. Particle identification (PID) is used to discriminate the type of charged hadron tracks: $\mathcal{R}(h|h') = \mathcal{L}(h)/(\mathcal{L}(h) + \mathcal{L}(h'))$ is defined as the ratio of the likelihoods for the h and h' hypotheses, where $\mathcal{L}(h)$ ($h = \pi, K, \text{ or } p$) is the combined likelihood derived from the ACC, TOF, and CDC dE/dx measurements [20]. $\mathcal{R}(p|\pi) > 0.9$ and $\mathcal{R}(p|K) > 0.9$ are required for protons. $\mathcal{R}(K|p) > 0.4$ and $\mathcal{R}(K|\pi) > 0.9$ are required for charged kaons. $\mathcal{R}(\pi|p) > 0.4$ and $\mathcal{R}(\pi|K) > 0.4$ are required for charged pions. $\mathcal{R}(e)$, a likelihood ratio for e and h identification formed from ACC, CDC, and ECL information [21], is required to be less than 0.9 for all charged tracks to remove electrons. For the typical momentum range of our SCS decays, the identification efficiencies of p, K , and π are 81.7%, 79.6%, and 96.9%, respectively.

A Λ_c^+ candidate for the CF decay is reconstructed from three tracks identified as p, K , and π , subject to a common-vertex fit. The χ^2 of the vertex fit is required to be less than 40 to reject background from incorrect combinations. The scaled momentum of the Λ_c^+ , defined as $x_p = p^*/\sqrt{E_{\text{cm}}^2/4 - M^2}$ [22], is required to be greater than 0.53 for all Λ_c^+ candidates to suppress the combinatorial background, especially from B -meson decays. Here, E_{cm} is the center-of-mass (CM) energy, while p^* and M are the momentum and invariant mass, respectively, of the Λ_c^+ candidates in the CM frame. All of these optimized selection criteria are taken from Ref. [23].

An ECL cluster not matching any track is identified as a photon candidate. Each photon candidate is required to have a ratio of energy deposited in the central 3×3 square of ECL cells to that deposited in the enclosing 5×5 square of cells of $E9/E25 > 0.8$ to reject neutral hadrons. An optimized figure-of-merit (FOM) study determines that the

energies of photon candidates must exceed 50 MeV and 110 MeV in the barrel and end cap regions of the ECL, respectively, for both photons from $\pi^0 \rightarrow \gamma\gamma$. For the $\eta \rightarrow \gamma_1\gamma_2$ decay, the γ_1 (γ_2) energies must exceed 220 (260) MeV, 480 (340) MeV, and 260 (360) MeV in the barrel, forward, and backward end caps, respectively. Two photon candidates are combined to form a π^0/η candidate, and a mass-constrained fit is performed for this candidate. The χ^2 value of the mass-constrained fit must be less than 7.5 and 4 for π^0 and η candidates, respectively, to suppress the background in which the two-photon invariant mass is far from π^0 and η nominal masses [9]. The momentum in the CM frame must be greater than 0.69 GeV/c and 0.82 GeV/c for π^0 and η candidates, respectively. All these requirements are optimized. An SCS Λ_c^+ candidate is reconstructed by combining a proton candidate with a π^0/η candidate. Again, x_p for the $\Lambda_c^+ \rightarrow p\pi^0/p\eta$ candidates is required to exceed 0.53. After applying all the selection criteria, about 0.8%, 1.4%, and 1.7% of the events in the signal region have multiple Λ_c^+ candidates for the $pK^-\pi^+$, $p\eta$, and $p\pi^0$ decays, respectively.

The SCS signal region in data is optimized with the control sample of $\Lambda_c^+ \rightarrow pK^-\pi^+$, as well as the Λ_c^+ mass sidebands to the hidden SCS signal region (i.e., the signal region is blinded), by optimizing the ratio $S/\sqrt{S+B}$, where S and B are the expected number of signal events for SCS decays in data and the number of background events normalized to the signal region, respectively. S is obtained via

$$S = \epsilon^{\text{MC}}(\Lambda_c^+ \rightarrow p\pi^0/p\eta) \times \frac{N^{\text{obs}}(\Lambda_c^+ \rightarrow pK^-\pi^+)}{\epsilon^{\text{MC}}(\Lambda_c^+ \rightarrow pK^-\pi^+)} \times \frac{\mathcal{B}(\Lambda_c^+ \rightarrow p\pi^0/p\eta) \times \mathcal{B}(\pi^0/\eta \rightarrow \gamma\gamma)}{\mathcal{B}(\Lambda_c^+ \rightarrow pK^-\pi^+)}, \quad (2)$$

where N^{obs} and ϵ^{MC} are the fitted Λ_c^+ events of data and the detection efficiency of the signal MC sample, respectively; $\mathcal{B}(\Lambda_c^+ \rightarrow p\pi^0/p\eta)$ are the branching fractions of 2.7×10^{-4} and 1.24×10^{-3} for $\Lambda_c^+ \rightarrow p\pi^0$ and $\Lambda_c^+ \rightarrow p\eta$, respectively [13]; and $\mathcal{B}(\Lambda_c^+ \rightarrow pK^-\pi^+)$ is the branching fraction of the CF decay [9].

IV. EFFICIENCY ESTIMATION AND FIT RESULTS

With the final selection criteria applied, the invariant mass distributions of $pK^-\pi^+$, $p\eta$, and $p\pi^0$ from data are shown in Figs. 2, 3, and 4, respectively. From the study of the topology of inclusive MC samples [19], no peaking backgrounds contribute to these mass distributions in the Λ_c^+ signal region.

For the CF mode, we fit the invariant mass distribution of $pK^-\pi^+$ displayed in Fig. 2 from 2.15 to 2.42 GeV/c² using the binned maximum likelihood fit with a bin width

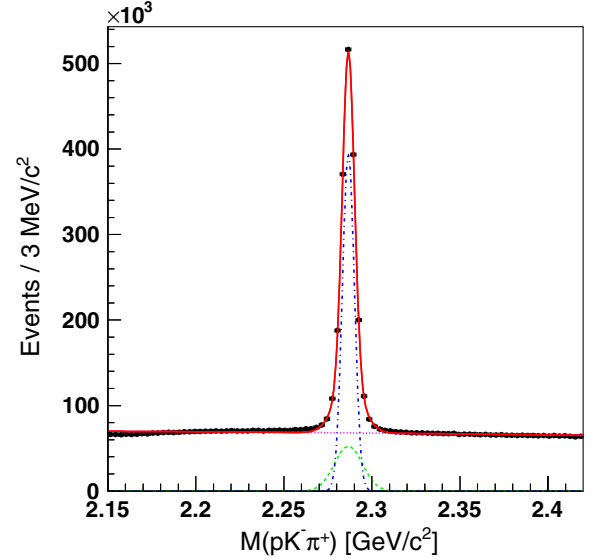


FIG. 2. Fit to the invariant mass distribution of $pK^-\pi^+$ from data. Black dots with error bars represent the data; the pink dashed line, the blue dash-dotted line, the green dashed line, and the red solid line represent the background contribution, the core Gaussian, tail Gaussian, and the total fit, respectively.

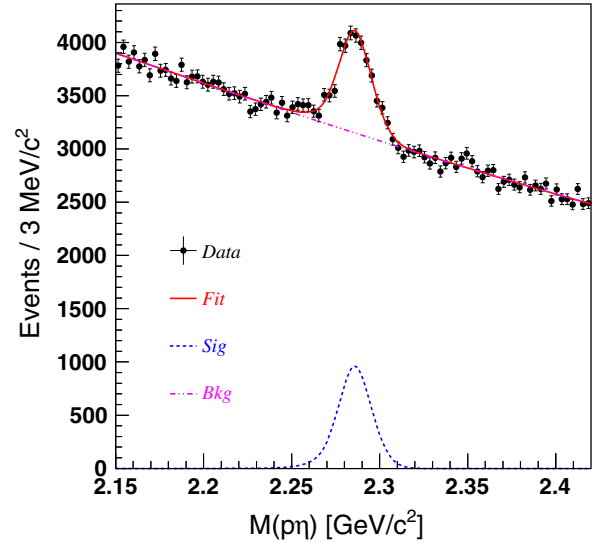


FIG. 3. Fit to the invariant mass distribution of $p\eta$ from data. Black dots with error bars represent the data; the magenta dash-dotted line, the blue dashed line, and the red solid line represent the background component, the signal, and the total fit, respectively.

of 3 MeV/c². A double-Gaussian function with the common mean value is used to model the signal events, and a second-order polynomial is used to model the background events. The parameters of the signal and background shapes are free in the fit. The reduced χ^2 value of the fit is $\chi^2/\text{ndf} = 87/82 = 1.06$, and the fitted number of signal events is 1476200 ± 1560 , where ndf is

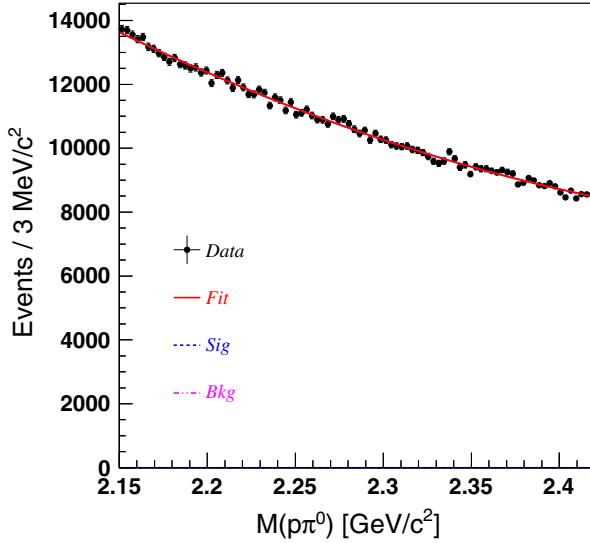


FIG. 4. Fit to the invariant mass distribution of $p\pi^0$. Black dots with error bars represent the data; the magenta dash-dotted line, the blue dashed line, and the red solid line represent the background component, the signal, and the total fit, respectively.

the number of degrees of freedom and the uncertainty is statistical only.

The Dalitz [24] distribution of $M^2(K^-\pi^+)$ versus $M^2(pK^-)$ in the signal region from data is shown in Fig. 5. The signal region is taken from 2.274 to 2.298 GeV/c^2 . We divide this into 120×120 pixels, with size $0.027 \text{ GeV}^2/c^4$ for $M^2(pK^-)$ and $0.016 \text{ GeV}^2/c^4$ for $M^2(K^-\pi^+)$. The number of background events has been subtracted using the normalized sidebands. The sideband regions are defined to be $(2.262, 2.274) \text{ GeV}/c^2$ and $(2.298, 2.310) \text{ GeV}/c^2$. A MC sample mixing four sub-channels of CF decay weighted with the corresponding branching fractions taken from Ref. [9] is used to assess the selection efficiency of the CF mode. The total number of reconstructed MC signal events is normalized to that of

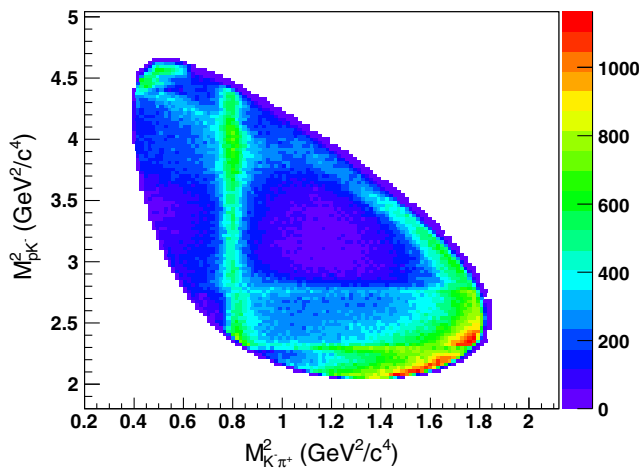


FIG. 5. Dalitz plot of the selected $\Lambda_c^+ \rightarrow pK^-\pi^+$ candidates.

signal candidates in data. We calculate the overall efficiency using the efficiency of each pixel. The formula is $\epsilon = \sum_i s_i / \sum_j (s_j / \epsilon_j)$, where $\sum_i s_i$ is the number of signal candidates in data, and s_j and ϵ_j are the number of signal events from data and the efficiency from the MC sample for each pixel, respectively. The efficiency of one pixel is obtained by dividing the number of events remaining in the signal MC sample by the number of generated events. The weighted efficiency for each bin is exhibited in Fig. 6, and the corrected efficiency for data is $(14.06 \pm 0.01)\%$.

An obvious Λ_c^+ signal peaking in the signal region of the $M(p\eta)$ spectrum is observed. We use the binned maximum likelihood method to fit the invariant mass distribution of $p\eta$ from 2.15 to 2.42 GeV/c^2 with a $3 \text{ MeV}/c^2$ bin width. A combined Gaussian and crystal ball (CB) [25] function with a common mean value models the signal, and a second-order polynomial models the background. The parameters of the signal and background line shapes are free in the fit. Figure 3 exhibits the distribution of the invariant mass of $p\eta$ and the corresponding fit result. The reduced χ^2 of the fit is $\chi^2/\text{ndf} = 102/83 = 1.23$, and the fitted number of signal events is 7734 ± 263 .

There is no significant excess observed in the signal region for $\Lambda_c^+ \rightarrow p\pi^0$. We fit $M(p\pi^0)$ with the binned maximum likelihood method; the fit result is shown in Fig. 4. The signal is modeled by a combined Gaussian and CB function with the common mean convolved with a Gaussian function; the background is described by a second-order polynomial. The parameters of the signal are fixed to MC-derived values, and the convolving Gaussian with width 2.1 MeV accounts for the difference in widths between data and MC for the $\Lambda_c^+ \rightarrow p\eta$ signal. The fitted number of signal events and the parameters of the background polynomial are free in the fit. The fitting range is from 2.15 to 2.42 GeV/c^2 , with a bin width of $3 \text{ MeV}/c^2$. The fitted number of signal events is 11 ± 140 ,

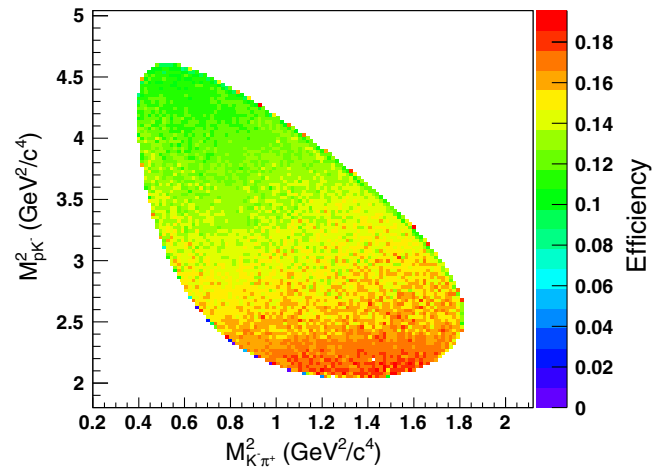


FIG. 6. Dalitz plot of efficiency distribution for $\Lambda_c^+ \rightarrow pK^-\pi^+$ decay.

which is consistent with zero. Thus, with a uniform prior probability density function, the estimation of a Bayesian upper limit is performed to obtain the 90% credibility level (C.L.) upper limit on the branching fraction of $\Lambda_c^+ \rightarrow p\pi^0$. The likelihood function is integrated from zero to the value that gives 90% of the total area. Before integrating, we include the systematic uncertainty (σ_{sys}) described below by convolving the likelihood distribution with a Gaussian whose width is equal to σ_{sys} . An upper limit on the branching fraction of 9.44×10^{-5} at 90% C.L. is set. The likelihood distribution as a function of the branching fraction, with the systematic uncertainty included, is displayed in Fig. 7.

To estimate the efficiencies of the two SCS decays, we take the ratio of the number of fitted signal events in the invariant mass distribution of $p\pi^0/p\eta$ to that of generated events from signal MC samples as the efficiency. We find $(8.28 \pm 0.03)\%$ and $(8.89 \pm 0.03)\%$ for $\Lambda_c^+ \rightarrow p\eta$ and $\Lambda_c^+ \rightarrow p\pi^0$, respectively. The uncertainties are statistical only.

V. SYSTEMATIC UNCERTAINTIES

Since the branching fraction is obtained from the ratio of the corresponding quantities in Eq. (1), some systematic uncertainties for $\Lambda_c^+ \rightarrow p\pi^0/p\eta$ cancel. The sources of systematic uncertainties include the fits of CF and SCS decays, PID, tracking efficiency, photon efficiency, the uncertainties of branching fractions of CF and $\pi^0/\eta \rightarrow \gamma\gamma$ decays, and the statistics of the signal MC samples.

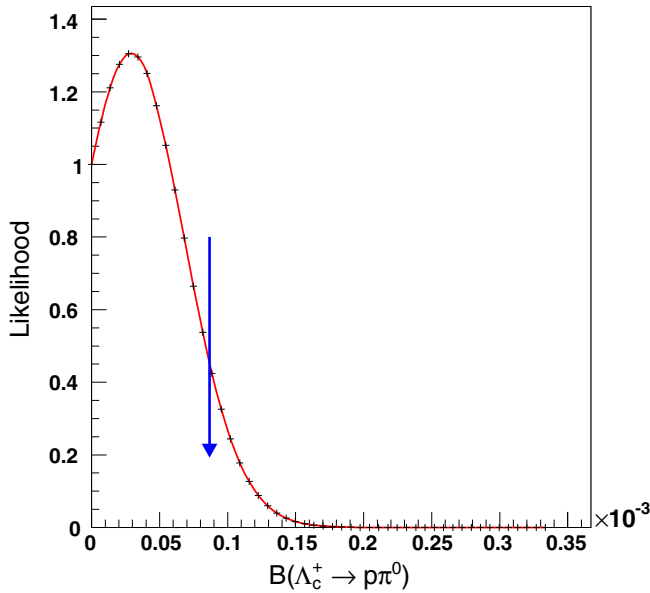


FIG. 7. The likelihood distribution as a function of the branching fraction for $\Lambda_c^+ \rightarrow p\pi^0$ with the systematic uncertainty included. The blue arrow refers to the 90% C.L. upper limit on the branching fraction.

To estimate the uncertainties from the fits of CF and SCS decays, we modify the signal and background functions, the bin width, and the fit range and refit. To evaluate the uncertainty from the signal function, the signal shape for $\Lambda_c^+ \rightarrow pK^-\pi^+/p\eta$ is fixed to that from the fit to the MC sample, while that for $\Lambda_c^+ \rightarrow p\pi^0$ is changed from a Gaussian and CB combined function to a double CB function. The uncertainty from the background line shape is assessed by using a first-order polynomial. Furthermore, we change the bin width to 2 MeV/ c^2 or 4 MeV/ c^2 , and adjust the fit range of the invariant mass spectrum to estimate the uncertainties from binning and fit range. The difference of branching fractions between the refitted and nominal conditions is taken as the uncertainty, which is 3.86% for $\Lambda_c^+ \rightarrow p\pi^0$ and 2.85% for $\Lambda_c^+ \rightarrow p\eta$, respectively.

The systematic uncertainties from PID and tracking efficiency of the proton cancel in the branching-fraction ratio. Systematic uncertainties of 1.6% and 1.2% are assigned for the K and π identification efficiencies, respectively, by studying a low-background control sample of D^* . The total systematic uncertainty from PID is 2.0%, the sum in quadrature of the individual uncertainties for K and π . From the study of the mid- to high-momentum track reconstruction efficiency in $D^* \rightarrow \pi D^0$ decay, the uncertainty of the efficiency for each charged track is 0.35%, resulting in a total uncertainty of 0.7% from tracking efficiency. We assign a 2% systematic uncertainty due to the photon efficiency per photon according to a study of radiative Bhabha events; the total systematic uncertainty from photon reconstruction is thus 4%.

The systematic uncertainties from the branching fractions of CF and $\pi^0/\eta \rightarrow \gamma\gamma$ are 5.1%, 0.034%, and 0.5% [9], respectively.

The systematic uncertainty from the size of the signal MC sample is estimated to be 0.34% and 0.35% for $\Lambda_c^+ \rightarrow p\pi^0$ and $\Lambda_c^+ \rightarrow p\eta$ decays, respectively.

The systematic uncertainties are summarized in Table I and give in total 7.8% and 7.4% for $\Lambda_c^+ \rightarrow p\pi^0$ and $\Lambda_c^+ \rightarrow p\eta$, respectively, which are obtained by assuming

TABLE I. The sources of the relative systematic uncertainties (%) on the branching fractions of $\Lambda_c^+ \rightarrow p\pi^0$ and $\Lambda_c^+ \rightarrow p\eta$ decays.

Source	$\Lambda_c^+ \rightarrow p\pi^0$	$\Lambda_c^+ \rightarrow p\eta$
Fit of signal decay	3.9	2.8
PID	2.0	2.0
Tracking efficiency	0.7	0.7
Photon efficiency	4.0	4.0
$B(\Lambda_c^+ \rightarrow pK^-\pi^+)$	5.1	5.1
$B(\pi^0/\eta \rightarrow \gamma\gamma)$	0.0	0.5
Statistics of signal MC samples	0.3	0.4
Total	7.8	7.4

all uncertainties are independent and therefore added in quadrature.

VI. CONCLUSION

We observe the decay $\Lambda_c^+ \rightarrow p\eta$. A significant Λ_c^+ signal is observed in the invariant mass distribution of $p\eta$ from data. Using the numbers of the fitted signal events of the $\Lambda_c^+ \rightarrow p\eta$ and $pK^-\pi^+$ models and the reconstruction efficiencies, the measured ratio of $\frac{\mathcal{B}(\Lambda_c^+ \rightarrow p\eta)}{\mathcal{B}(\Lambda_c^+ \rightarrow pK^-\pi^+)} = [2.258 \pm 0.077(\text{stat}) \pm 0.122(\text{syst})] \times 10^{-2}$ is obtained via Eq. (1). With the independently measured value of $\mathcal{B}(\Lambda_c^+ \rightarrow pK^-\pi^+)$ [9], we extract a branching fraction of $\mathcal{B}(\Lambda_c^+ \rightarrow p\eta) = [1.42 \pm 0.05(\text{stat}) \pm 0.11(\text{syst})] \times 10^{-3}$, which is consistent with both the latest published measurement of $(1.24 \pm 0.30) \times 10^{-3}$ [13], but with much improved precision, and with theoretical predictions within 1.3σ [11,12].

We see no obvious signal excess in the distribution of $M(p\pi^0)$, and so we set an upper limit on the ratio of the branching fractions $\frac{\mathcal{B}(\Lambda_c^+ \rightarrow p\pi^0)}{\mathcal{B}(\Lambda_c^+ \rightarrow pK^-\pi^+)}$ at a 90% C.L. of 1.273×10^{-3} . From this, we extract an upper limit on the branching fraction of $\mathcal{B}(\Lambda_c^+ \rightarrow p\pi^0) < 8.0 \times 10^{-5}$ at a 90% C.L., more than 3 times more stringent than the best current upper limit of 2.7×10^{-4} [13]. The measured $\mathcal{B}(\Lambda_c^+ \rightarrow p\eta)$ is at least an order of magnitude larger than $\mathcal{B}(\Lambda_c^+ \rightarrow p\pi^0)$, which is consistent with the theoretical prediction of an internal W -emission mechanism involving an s quark in $\Lambda_c^+ \rightarrow p\eta$ [11].

ACKNOWLEDGMENTS

We thank the KEKB group for the excellent operation of the accelerator; the KEK cryogenics group for the efficient operation of the solenoid; the KEK computer group and the Pacific Northwest National Laboratory (PNNL) Environmental Molecular Sciences Laboratory (EMSL) computing group for strong computing support; and the National Institute of Informatics and Science Information NETwork 5 (SINET5) for valuable network support. We acknowledge support from the Ministry of Education, Culture, Sports, Science, and Technology (MEXT) of

Japan, the Japan Society for the Promotion of Science (JSPS), and the Tau-Lepton Physics Research Center of Nagoya University; the Australian Research Council including Grants No. DP180102629, No. DP170102389, No. DP170102204, No. DP150103061, and No. FT130100303; the Austrian Science Fund (FWF); the National Natural Science Foundation of China under Contracts No. 11435013, No. 11475187, No. 11521505, No. 11575017, No. 11675166, No. 11705209, No. 11761141009, No. 11975076, and No. 12042509; the Key Research Program of Frontier Sciences, Chinese Academy of Sciences (CAS), Grant No. QYZDJ-SSW-SLH011; the CAS Center for Excellence in Particle Physics (CCEPP); the Shanghai Pujiang Program under Grant No. 18PJ1401000; the Ministry of Education, Youth and Sports of the Czech Republic under Contract No. LTT17020; the Carl Zeiss Foundation, the Deutsche Forschungsgemeinschaft, the Excellence Cluster Universe, and the VolkswagenStiftung; the Department of Science and Technology of India; the Istituto Nazionale di Fisica Nucleare of Italy; the National Research Foundation (NRF) of Korea Grants No. 2016R1D1A1B01010135, No. 2016R1D1A1B02012900, No. 2018R1A2B3003643, No. 2018R1A6A1A06024970, No. 2018R1D1A1B07047294, No. 2019K1A3A7A09033840, and No. 2019R1I1A3A01058933; the Radiation Science Research Institute, the Foreign Large-size Research Facility Application Supporting Project, the Global Science Experimental Data Hub Center of the Korea Institute of Science and Technology Information and KREONET/GLORIAD; the Polish Ministry of Science and Higher Education and the National Science Center; the Ministry of Science and Higher Education of the Russian Federation, Agreement No. 14.W03.31.0026; University of Tabuk research grants No. S-1440-0321, No. S-0256-1438, and No. S-0280-1439 (Saudi Arabia); the Slovenian Research Agency; Ikerbasque, the Basque Foundation for Science, Spain; the Swiss National Science Foundation; the Ministry of Education and the Ministry of Science and Technology of Taiwan; and the United States Department of Energy and the National Science Foundation.

[1] K. K. Sharma and R. C. Verma, *Phys. Rev. D* **55**, 7067 (1997).
 [2] M. A. Ivanov, J. G. Korner, V. E. Lyubovitskij, and A. G. Rusetsky, *Phys. Rev. D* **57**, 5632 (1998).
 [3] T. Uppal, R. C. Verma, and M. P. Khanna, *Phys. Rev. D* **49**, 3417 (1994).
 [4] P. Zenczykowski, *Phys. Rev. D* **50**, 402 (1994).
 [5] Y. Kohara, *Nuovo Cimento A* **111**, 67 (1998), <https://link.springer.com/article/10.1007/BF03185573>.

[6] M. Niiyama *et al.* (Belle Collaboration), *Phys. Rev. D* **97**, 072005 (2018).
 [7] B. Andersson, G. Gustafson, G. Ingelman, and T. Sjöstrand, *Phys. Rep.* **97**, 31 (1983).
 [8] B. Andersson, G. Gustafson, and T. Sjöstrand, *Phys. Scr.* **32**, 574 (1985).
 [9] P. A. Zyla *et al.* (Particle Data Group), *Prog. Theor. Exp. Phys.* (2020), 083C01.

- [10] C. D. Lü, W. Wang, and F. S. Yu, *Phys. Rev. D* **93**, 056008 (2016).
- [11] H. Y. Cheng, X. W. Kang, and F. R. Xu, *Phys. Rev. D* **97**, 074028 (2018).
- [12] J. Q. Zou, F. R. Xu, G. B. Meng, and H. Y. Cheng, *Phys. Rev. D* **101**, 014011 (2020).
- [13] M. Ablikim *et al.* (BESIII Collaboration), *Phys. Rev. D* **95**, 111102 (2017).
- [14] S. Kurokawa and E. Kikutani, *Nucl. Instrum. Methods Phys. Res., Sect. A* **499**, 1 (2003), and other papers included in this volume; T. Abe *et al.*, *Prog. Theor. Exp. Phys.* (2013), 03A001, and references therein.
- [15] A. Abashian *et al.* (Belle Collaboration), *Nucl. Instrum. Methods Phys. Res., Sect. A* **479**, 117 (2002); also, see detector section in J. Brodzicka *et al.*, *Prog. Theor. Exp. Phys.* **2012**, 04D001 (2012).
- [16] T. Sjostrand, S. Mrenna, and P. Skands, *Comput. Phys. Commun.* **178**, 852 (2008).
- [17] D. J. Lange, *Nucl. Instrum. Methods Phys. Res., Sect. A* **462**, 152 (2001).
- [18] R. Brun *et al.*, GEANT3: User's guide GEANT3.10, GEANT3.11, CERN Report No. DD/EE/84-1, 1984.
- [19] X. Y. Zhou, S. X. Du, G. Li, and C. P. Shen, *Comput. Phys. Commun.* **258**, 107540 (2021).
- [20] E. Nakano, *Nucl. Instrum. Methods Phys. Res., Sect. A* **494**, 402 (2002).
- [21] K. Hanagaki, H. Kakuno, H. Ikeda, T. Iijima, and T. Tsukamoto, *Nucl. Instrum. Methods Phys. Res., Sect. A* **485**, 490 (2002).
- [22] We used units in which the speed of light is $c = 1$.
- [23] S. B. Yang *et al.* (Belle Collaboration), *Phys. Rev. Lett.* **117**, 011801 (2016).
- [24] R. H. Dalitz, *Philos. Mag. Ser. 5* **44**, 1068 (1953).
- [25] J. E. Gaiser, Ph. D. thesis, Stanford Linear Accelerator Center, Stanford University, Report No. SLAC-R-255, 1982.